

## 1.4 ANGULAR DEPENDENCE OF CLOUD PROPERTY RETRIEVALS FROM SATELLITE DATA

J. Kirk Ayers\*, Rabindra Palikonda, and Mandana M. Khaiyer  
Analytical Services & Materials Inc  
Hampton, Virginia

Patrick Minnis, Louis Nguyen, and William L. Smith, Jr.  
National Aeronautics and Space Administration  
Langley Research Center  
Hampton, Virginia

Robert Arduini,  
Science Applications International Corporation  
Hampton, Virginia

### 1.0 INTRODUCTION

Satellite cloud retrievals and products are the basis for GCM validation and future assimilation over large spatial domains. Cloud retrievals and products are derived from many satellite instruments and platforms. Geosynchronous orbiting satellites provide the capability for performing coincident retrievals of cloud properties from different pairs of viewing angles. The amount of variation in a given retrieved property with viewing angles is a measure of the accuracy of the retrieval because, ideally, the variation should be zero. Thus, pairs of measurements from two or more different angles can provide an assessment of cloud retrieval algorithm performance. Some of the difference may be due to 3-D cloud structure and variances in the phase functions that are not captured in the simple retrieval models. By viewing the same clouds simultaneously from different angles, it is possible to estimate the model uncertainties caused by 3-D effects and model assumptions. By altering the model characteristics that minimize parameter differences, due to view angles, it is possible to make improvements to the model and minimize the impacts of the model assumptions. This study utilizes dual coverage area GOES-12 (75° W), GOES-10 (135° W) multi-spectral data from April, July and October 2004, and January 2005. Future analyses will compare GOES-11 (~115° W) data with GOES-10 and GOES-12 during July 2005. The Visible Infrared Solar-infrared Split-window Technique is used to retrieve cloud optical depth, phase, particle size, water path and height and temperature. Angular biases of cloud properties are quantified by scattering angle, diurnally and seasonally. Modification of water droplet distribution models are tested by changing particle size distributions. The results are compared to surface observations of liquid water path.

### 2.0 METHODOLOGY

This study utilizes the Visible Infrared Solar-infrared Split-window Technique (VISST) to determine cloud properties. VISST is a 4-channel model-matching

method for plane parallel clouds, (Minnis et al., 2001). It utilizes parameterizations of radiative transfer calculations for 7 water and 9 ice crystal size distributions (Minnis et al., 1998) to estimate theoretical radiances that are matched with 4-km GOES-10 (G-10), GOES-12 (G-12), or GOES-11 (G-11) 0.65, 3.9, and 10.8  $\mu\text{m}$  radiances to estimate several cloud properties. Additionally, the 12.0- $\mu\text{m}$  channel, missing on the G-12, is used in the analysis of the G-10 images. Atmospheric profiles of temperature and humidity derived from 40-km Rapid Update Cycle (RUC-2) hourly analyses are used to estimate the skin temperature, calculate cloud height from the derived cloud temperature, and account for atmospheric absorption in each channel. Surface type is based on the IGBP 10-minute resolution surface map. Clear-sky reflectances and ice and snow masks developed for the Clouds and the Earth's Radiant Energy System (CERES) program are used for additional surface characterization (Trepte et al., 1999). The primary products produced by VISST are pixel-level retrievals of micro and macro physical cloud properties including cloud phase, optical depth ( $\tau$ ), effective droplet radius ( $R_e$ ) or effective ice particle diameter ( $D_e$ ), liquid water path (LWP) or ice water path (IWP), and cloud height and temperature, (Minnis et al., 2004). A secondary product of VISST is a grid-level average of the pixel-level data. The grid resolution can be specified by the user and was set to 0.5° equal angle for this study.

This study uses coincident G-10 and G-12 data from April, July, and October 2004 and from January 2005. These months were selected to account for seasonal variation in sun angle and cloud properties. The data from each month were individually screened to select 3 days per month to provide a near equal mix of ice and water clouds. The area selected for analysis, shown in Fig. 1, is bounded by 50°N, 90°W and 25°N, 105°W. This area provides optimal satellite observation overlap. In addition, tri-view data from GOES-10, GOES-11, and GOES-12 from selected days during July 2005 will be analyzed in the future.

Data from the satellite overlap region were analyzed with the VISST and the results were averaged into gridded network Common Data Format (NetCDF) files. The G-10 and G-12 results were spatially and temporally matched and filtered to categorize clouds as primarily (>90%) ice or water phase. Only grid boxes

---

\* Corresponding Author Address: J. K. Ayers, AS&M, Inc., 1 Enterprise Parkway Hampton, VA 23666; e-mail: j.k.ayers@larc.nasa.gov

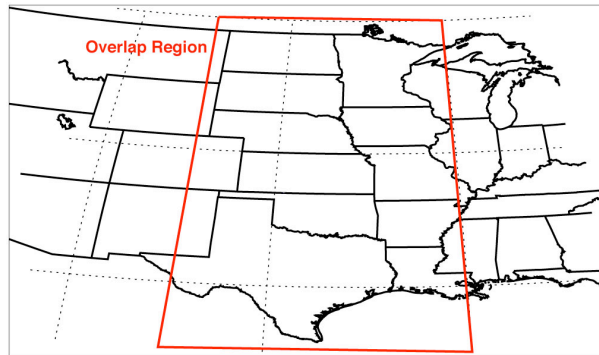


Figure 1. Overview of the satellite observation overlap analysis region.

having 100% cloud cover with a primary (>90%) phase were included in this study. After filtering for  $\tau \leq 32$ , regression analyses of various properties was performed and evaluated for agreement. Finally, an attempt was made to identify factors contributing to poor agreement.

### 3.0 RESULTS

Matched grid box averages of water cloud  $\tau$  taken at 1845 UTC are shown in Figure 2. As shown in the figure, the agreement is very good with a correlation coefficient of 0.92 and a bias of -1.06. The differences seen at larger optical depths are primarily related to effects of scattering angle and idealized models. Although not shown, the agreement between the VISST-derived values of  $Re$  is also relatively good. Generally,  $Re$  retrieved from G-10 is greater than that from G-12 for January and October, but the reverse is true for April and July. The combination of the monthly data nearly cancels the monthly biases leading to a total bias of only 0.45  $\mu\text{m}$ , or 5%. The hour, 1845 UTC, was

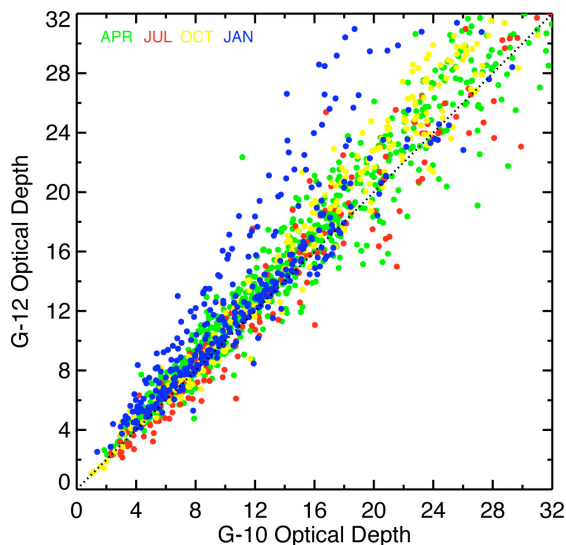


Figure 2. Comparison of VISST derived water cloud optical depth derived from G-10 and G-12.

selected because it is the image time nearest to local solar noon for this region. At local solar noon both satellites view the center of the region at nearly identical scattering angles providing the optimum comparison conditions. Similar comparisons were performed using data taken from 1415 to 2245 UTC to determine the effect of scattering angle differences. A summary of monthly mean  $\tau$  and  $Re$  for water cloud retrievals and their associated biases and RMS errors are shown in Fig. 3. As shown in Fig. 3a, the G10 VISST derived mean  $\tau$  ranges from 10 to 20, with an associated monthly maximum bias of -3.5 (-19%) relative to  $\tau$  from G12 (Fig. 3b). The monthly RMS errors (Fig. 3c) range from ~1.5 to ~5 (28%). The minimum bias and RMS errors occur near 1845 UTC, as expected. Except for April, the G10 optical depth tends to be larger during the afternoon than in the morning. Similarly, the bias is more negative in the morning. The overall mean optical depth for G10 was 15.7 with a mean bias of 0.86 and an RMS error of 1.4 (10%). Figure 3d shows that the monthly  $Re$  means range from 7 to 14  $\mu\text{m}$ , with a monthly maximum bias (Fig. 3e) of ~4.5  $\mu\text{m}$  at 2245 UTC during January when the sun is in near-terminator conditions. Otherwise, except at 1645 UTC during October, the biases are typically less than 2.5  $\mu\text{m}$ . Both the mean G-10 effective radii and the biases increase from morning to afternoon. The monthly RMS errors (Fig. 3f) range from 0.5 to ~5.0  $\mu\text{m}$ . The overall mean  $Re$  from G-10 data was 10.8  $\mu\text{m}$  with a mean bias of 0.28  $\mu\text{m}$  and an RMS error of 1.55  $\mu\text{m}$  (15%). The G10 mean cloud height of 1.99 km differed from its G12 counterpart by only 0.01 km. On a monthly hourly basis, water cloud height RMS differences are typically < 10% but can be as large as 27% (corresponding to a 0.08 km difference). Mean biases were typically less than 0.04 km. On average, the RMS difference between the matched pairs was 0.05 km (2.5%). The LWP analysis yielded a mean of 120  $\text{gm}^{-2}$  for G10 with a mean bias of 2.6  $\text{gm}^{-2}$  relative to G12. The mean RMS difference for the entire dataset is 19.5  $\text{gm}^{-2}$  (16%).

Ice cloud  $\tau$  values retrieved at 1845 UTC for the 4 months are compared in Fig. 4. The overall agreement in ice cloud  $\tau$  at 1845 UTC is fair with a bias of 1.5 (13%) and an RMS difference of 3.9. The G10 De mean (not shown) agrees very well with the G12 values. The overall De bias is only -0.18  $\mu\text{m}$  and the RMS difference is 8.2  $\mu\text{m}$  (~11%). These differences vary considerably with time of day. Compared to G-12, the mean G-10 ice cloud  $\tau$  ranges from 4 to 16, with associated monthly biases from -4 to 4. The monthly ice cloud RMS differences in  $\tau$  range from ~3 to ~6. Even though the bias is larger than that derived from water clouds, the minimum occurs at 1845 UTC, as expected. The overall mean  $\tau$  for G10 was 12.0 with a mean bias of 0.2 and an RMS difference of 2.2 (19%) relative to the G-12 values. Both water and ice cloud optical depths are larger during morning than in the afternoon, with values increasing again during late afternoon. The biases follow a similar cycle. The monthly mean De from G-10 ranges from 30 to 90  $\mu\text{m}$ . Excluding the near-terminator times in January and October, the values

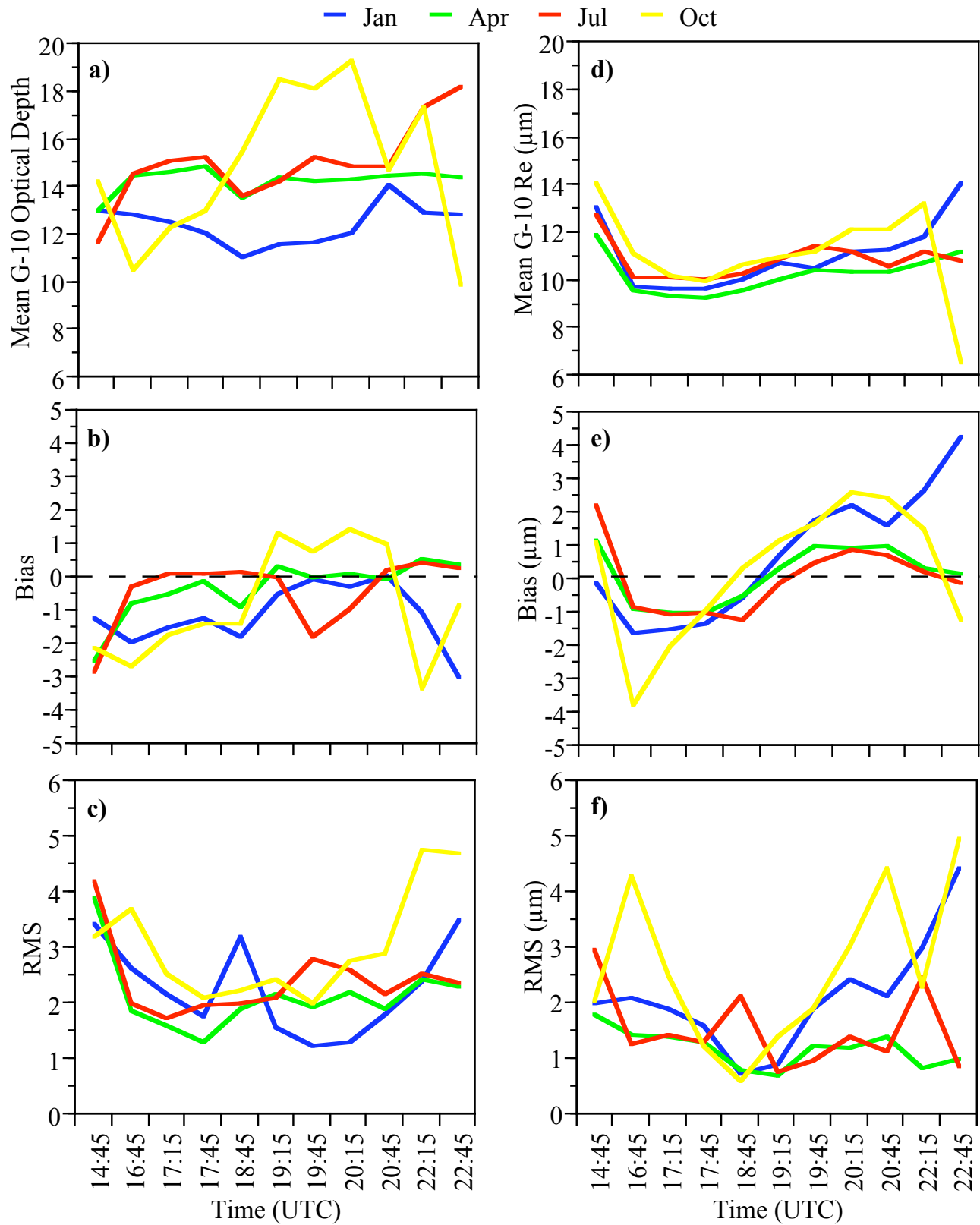


Figure 3. Summary of VISST derived G-10 hourly water cloud mean  $\tau$  and Re with associated biases and RMS errors from comparison to G-12 retrievals for the 4 months studied.

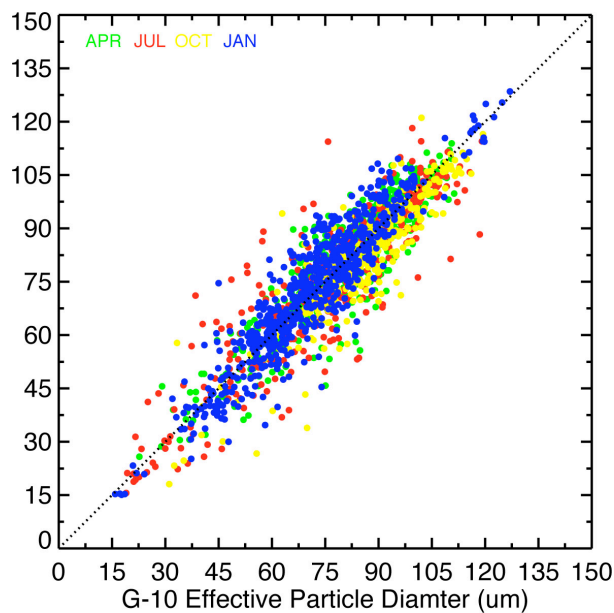


Figure 4. Comparison of VISST derived ice cloud optical depth derived from G-10 and G-12.

range from 70 to 87  $\mu\text{m}$ . The mean hourly differences between De from G-10 and G-12 are quite small at the near-terminator hours and as large as  $-23 \mu\text{m}$  at 1645 UTC during October. The monthly RMS differences in De range from 7.5 to 30  $\mu\text{m}$  with the greatest values found at the near-terminator hours and at 1645 and 2045 UTC during October. The overall mean De for G-10 was 68.5  $\mu\text{m}$  with a mean bias of  $-3.5 \mu\text{m}$  and an RMS error of 7.5  $\mu\text{m}$  (10%). The G-10-derived mean ice cloud height (not shown) of 7.58 km was 0.37 km lower, on average, than the G-10 values with an RMS difference of 0.44 km (5.6%). Ice cloud height instantaneous RMS differences are typically less than 10% except during January when at some hours they increase to as much as 40%, presumably due to the occurrence of thin clouds over snow fields or multi-layer clouds. Mean biases are generally less than 0.5 km. The IWP analysis yielded a mean of  $321 \text{ gm}^{-2}$  from G10 with a mean bias of  $-3.2 \text{ gm}^{-2}$  and a mean RMS difference of  $64.8 \text{ gm}^{-2}$  (20%).

#### 4.0 DISCUSSION

Although the optical depths shown are limited to 32, the results are similar for optical depths up to 128. The calculated instantaneous RMS errors reflect spatial sampling errors, combined with random errors from actual versus true model variations and 3-D cloud structure. The hourly mean bias errors are the best measure of uncertainties due to angular effects, including those from model assumptions and 3-D cloud structure.

The variation of the biases with UTC arises from the systematic changes in scattering angle. Pairs of scattering angles at selected hours for each month are shown in Fig. 5. The angles observed after 1845

UTC almost mirror those before 1845 UTC. The angles at 1845 UTC are not identical, which may explain the lack of unbiased retrievals. The biases change systematically from morning to afternoon due to the angle reversal. The larger biases observed at 1645 and 2045 UTC during October are likely due to the extreme angle pairs that occur at those times. One of the angles ( $177^\circ$ ) is very close to the direct backscatter position while the other is close to  $118^\circ$ . The water droplet scattering phase functions are very sensitive to the assumed droplet size distribution at certain angles, especially near the direct backscatter (Arduini et al., 2005). Cloud sides are most illuminated at large scattering angles, enhancing 3-D effects. The ice crystal phase function is extremely sensitive to particle shape around  $177^\circ$ , so any deviation from the assumed shape (hexagonal columns) is likely to cause extreme errors in the retrieval at the backscatter angles (Chepfer et al., 2002).

The extreme RMS values seen at the near-terminator hours are likely due to 3-D effects because the longer shadows and greater retro-reflectance produced at those times are more likely to cause greater deviations from the plane-parallel theory used in the VISST parameterizations than at any other times. This is especially true for the ice clouds that have more potential for long shadows and cloud sides. Apparently, the increase in De that would be caused by shadows is more than balanced by the decrease in De that should result from viewing the sunlit cloud sides at low sun angles. The scattering phase functions are similar for both views leading to small biases at these times. Despite the differences due to forward and backscatter viewing conditions at particular times, the biases tend to be canceled out if averaged over the course of the day. The water cloud errors are likely due to a variety of sources including 3-D effects, the assumed droplet size

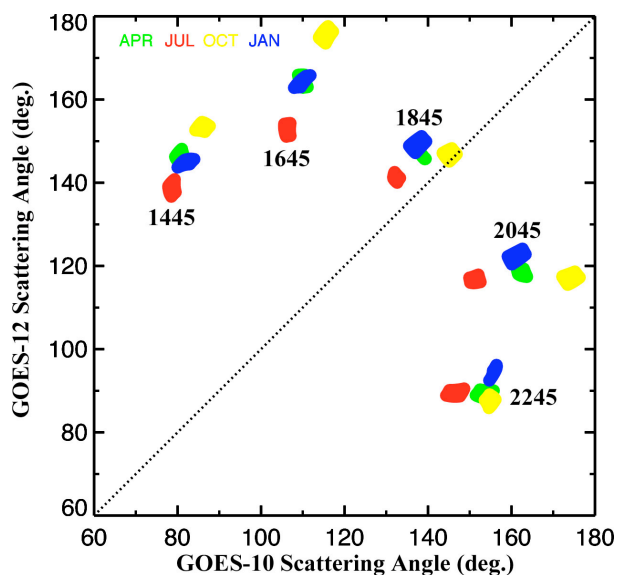


Figure 5. Hourly progression of matched scattering angle, color-coded by month of occurrence.

distribution, and, spatial and temporal mismatches. Preliminary results from Khaiyer et al. (2005) and Arduini et al. (2005) indicate that a broader size distribution could reduce the overall bias errors in LWP and Re substantially at each hour.

The observed errors in ice cloud optical depth retrievals are nearly twice as large as those from water clouds. Potentially, the use of other ice crystal models may lead to improved results from ice clouds as suggested by the dramatic errors at 1645 and 2045 UTC during October. Retrievals from ice clouds are subject to more errors than water clouds due to the effects of multi-layered clouds. The observed radiances can produce mixed ice and water signals that vary with the viewing angle.

## 5. VALIDATION

In order for satellite derived cloud macro and microphysical properties to be used for model assimilation they must be validated by use of in-situ or other objective measurements. To begin the validation process and investigate the effect of varying theoretical parameterizations VISST derived LWP was compared to LWP values derived from microwave radiometer (MWR) measurements collected at the ARM Southern Great Plains Central Facility (CF). The comparison was effected by matching an average of VISST pixel values in a 10-km radius centered on the CF with MWR measurements matched to the satellite observation time. As shown in Fig. 6 (blue points and fit), the initial comparison (G-10), using the VISST nominal effective droplet variance of 0.1, demonstrated fair agreement. The LWP values derived from VISST are overestimated as compared to those derived from the MWR. This overestimation leads to a significant bias ( $122.4 \text{ g/m}^2$ ) and a percent difference of  $\sim 93\%$ . In an attempt to improve the agreement the VISST droplet effective variance was changed to 0.2 (MOD20) and the comparison was redone (Figure 6., red points and fit). It is evident that for this comparison the MOD20-derived values are much closer to those derived from the MWR. The bias and percent difference are both decreased by  $\sim 70\%$ . The marked improvement in this comparison suggests that the VISST effective droplet variance should be changed to the MOD20 value. To further test the use of MOD20 a similar comparison was done using G-12 VISST derived LWP values (not shown). The use of MOD20 in the G-12 analysis leads to a  $\sim 20\%$  increase in the bias and percent difference. This increase contradicts the findings from the G-10 analysis and demonstrates the need for additional evaluation.

## 6. CONCLUSIONS

The VISST cloud properties derived from GOES data can be biased by angular effects. Differences between two satellite views can be as large as 15% for water clouds and as large as 20% for ice clouds at certain sets of angles or times of day. The actual true bias relative to the real optical depth or particle size is likely to be smaller than the difference between the two satellites

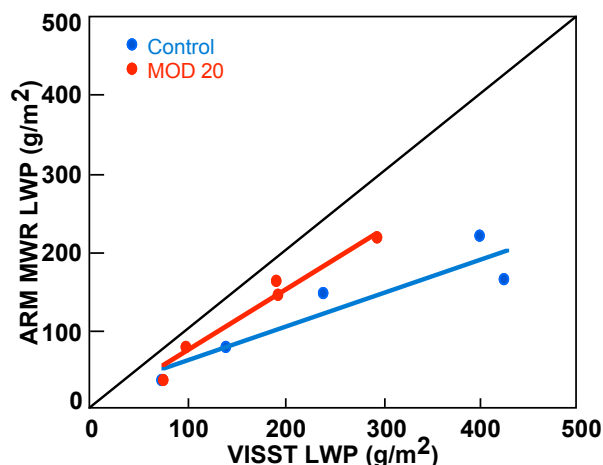


Figure 6. Comparison of October 2004 G-10 VISST and ARM Microwave Radiometer derived LWP. The VISST standard particle size effective variance (0.10) is shown in blue. The results derived using an effective variance of 0.2 (MOD20) is shown in red.

because they can be biased in different directions from the true value. Representation of the diurnal cycle of cloud properties from geostationary satellites can be affected by these biases. However, calculation of daily averaged cloud properties is generally good. Potentially the calculation of cloud properties may be improved through the use of varying particle size distributions and improved ice crystal models. The comparison of cloud retrievals from G-10 and G-12 show agreement for both ice and water clouds, that is consistent with observations from surface-satellite comparisons (e.g., Dong et al. 2002). The errors in the retrievals of water cloud properties are smaller, as expected, due to simpler particle shapes and cloud uniformity. The error in retrieval of ice cloud properties was larger, as expected, due to more complex particle shapes and variation from cloud to cloud. Retrieval of thin cirrus cloud properties, which is highly dependent on accurate characterization of the scene background, could also be a major source of error.

## 7. FUTURE WORK

The analysis domain will be extended to provide additional scattering angle pairs to more adequately quantify angular biases. It will be expanded to include night time observations, new algorithms, and G-11 analysis. Additional water droplet distribution models and ice crystal phase functions will be implemented and tested to evaluate their effect on cloud retrievals. The cloud retrievals will be evaluated to determine seasonal and diurnal cloud property variation. Three dimensional effects will be isolated by restricting samples by homogeneity of the scenes. Finally, validation studies using in-situ measurements from ARM and other sites will be used to verify the cloud retrievals.

## 8. REFERENCES

- Minnis, P., et al., 2001: A near-real time method for deriving cloud and radiation properties from satellites for weather and climate studies. *Proc. AMS 11<sup>th</sup> Conf. Satellite Meteor. and Oceanogr.*, Madison, WI, October 15-18.
- Minnis, P., D. P. Garber, D. F. Young, R. F. Arduini, and Y. Takano, 1998: Parameterization of reflectance and effective emittance for satellite remote sensing of cloud properties. *J. Atmos. Sci.*, 55, 3313-3339.
- Trepte, Q., Y. Chen, S. Sun-Mack, P. Minnis, D. F. Young, B. A. Baum, and P. W. Heck, 1999: Scene identification for the CERES cloud analysis subsystem. *Proc. AMS 10<sup>th</sup> Conf. Atmos. Rad.*, Madison, WI, June 28 – July 2, 1999, 169-172.
- Minnis, P., L. Nguyen, W. L. Smith, Jr., M. M. Khaiyer, R. Palikonda, D. A. Spangenberg, D. R. Doelling, D. Phan, G. D. Nowicki, P. W. Heck, and C. Wolff, 2004: Real-time cloud, radiation, and aircraft icing parameters from GOES over the USA. *Proc. 13<sup>th</sup> AMS Conf. Satellite Oceanogr. and Meteorol.*, Norfolk, VA, Sept. 20-24, CD-ROM, P7.1.
- Arduini, R. F., P. Minnis, W. L. Smith, Jr., J. K. Ayers, M.M. Khaiyer, and P.W. Heck: Sensitivity of Satellite-Retrieved Cloud Properties to the Effective Variance of Cloud Droplet Size Distribution. *Proc. of the 15<sup>th</sup> Annual ARM Science Team Meeting*, Daytona Beach, FL, March 14 – 18, 2005
- Chepfer, H., P. Minnis, D. F. Young, L. Nguyen, and R. F. Arduini, 2002: Estimation of cirrus cloud effective ice crystal shapes using visible reflectances from dual-satellite measurements. *J. Geophys. Res.*, **107 (D23)**, 10.1029/2000JD000240.
- Khaiyer, M. M., P. Minnis, R. F. Arduini, P. W. Heck, R. Palikonda, J. K. Ayers, D. N. Phan, and W. L. Smith, Jr.: Comparison of Cloud Liquid Water Paths over ARM SGP Using Satellite and Surface Data: Validation of New Models. *Proc. of the 15<sup>th</sup> Annual ARM Science Team Meeting*, Daytona Beach, FL, March 14 – 18, 2005
- Dong, X., P. Minnis, G. G. Mace, W. L. Smith, Jr., M. Poellot, R. T. Marchand, and A. D. Rapp, 2002: Comparison of stratus cloud properties deduced from surface, GOES, and aircraft data during the March 2000 ARM Cloud IOP. *J. Atmos. Sci.*, 59, 3256-3284.

## ACKNOWLEDGEMENTS

This research was sponsored by ITF No. 214216-A-Q1 from Pacific Northwest National Laboratory.